Mapping the dust in the Milky Way in 3D - structure of the Orion, Cygnus X, Taurus and Perseus star-forming regions

Thavisha Dharmawardena

Max Planck Institute for Astronomy – Gaia Group

dharmawardena@mpia.de

Co-Is: Coryn Bailer-Jones, Morgan Fouesneau, Dan Foreman-Mackey

Max-Planck-Institut für Astronomie Heidelberg

Max Planck Institute for Astronomy Heidelberg

Astronomische Gesellschaft Annual meeting – EScience und Virtual Observatory session

17.09.2021

esa

gaia

Why do we care about dust?...

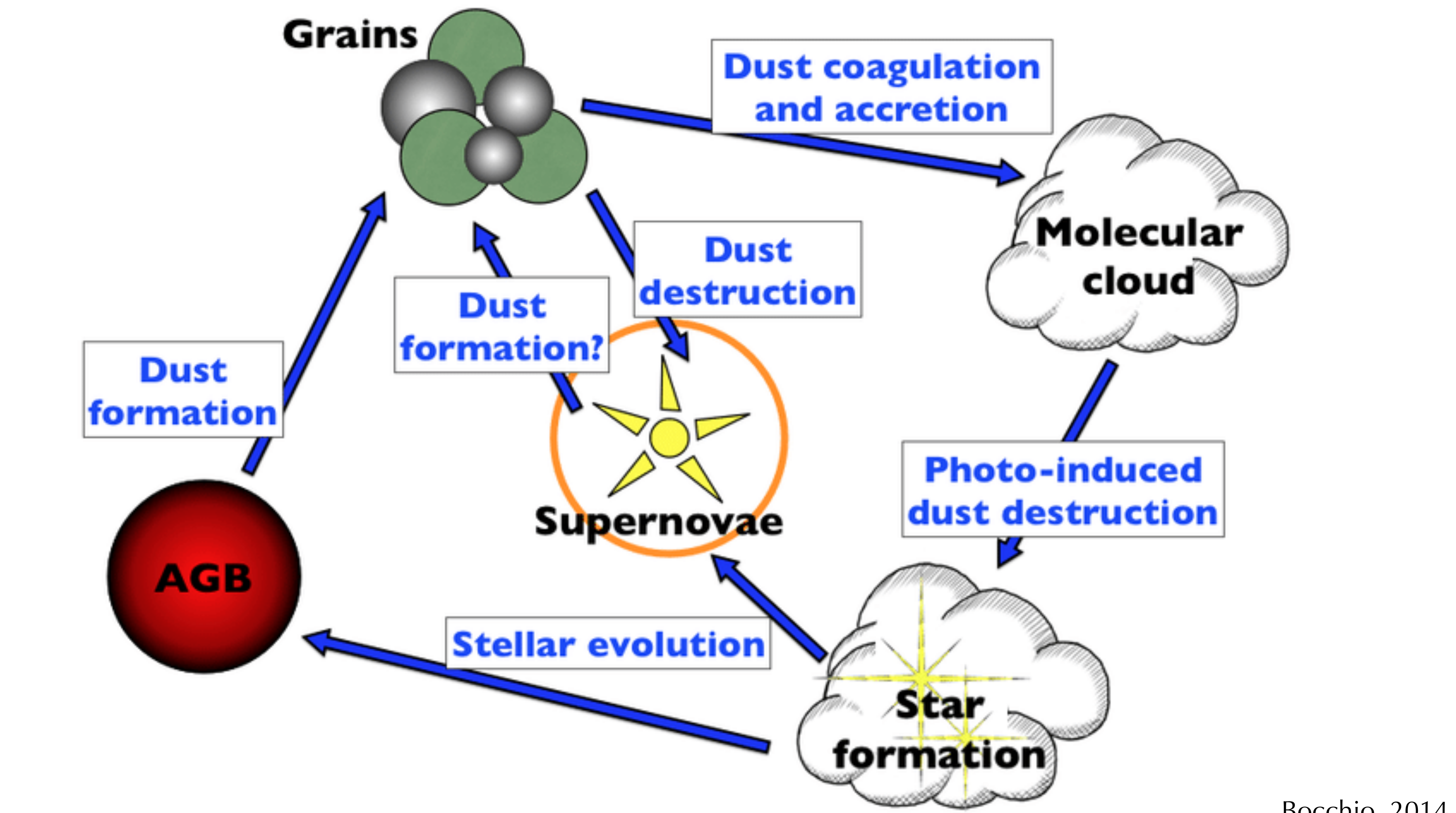

Bocchio, 2014

Why do we care about the spatial distribution of dust

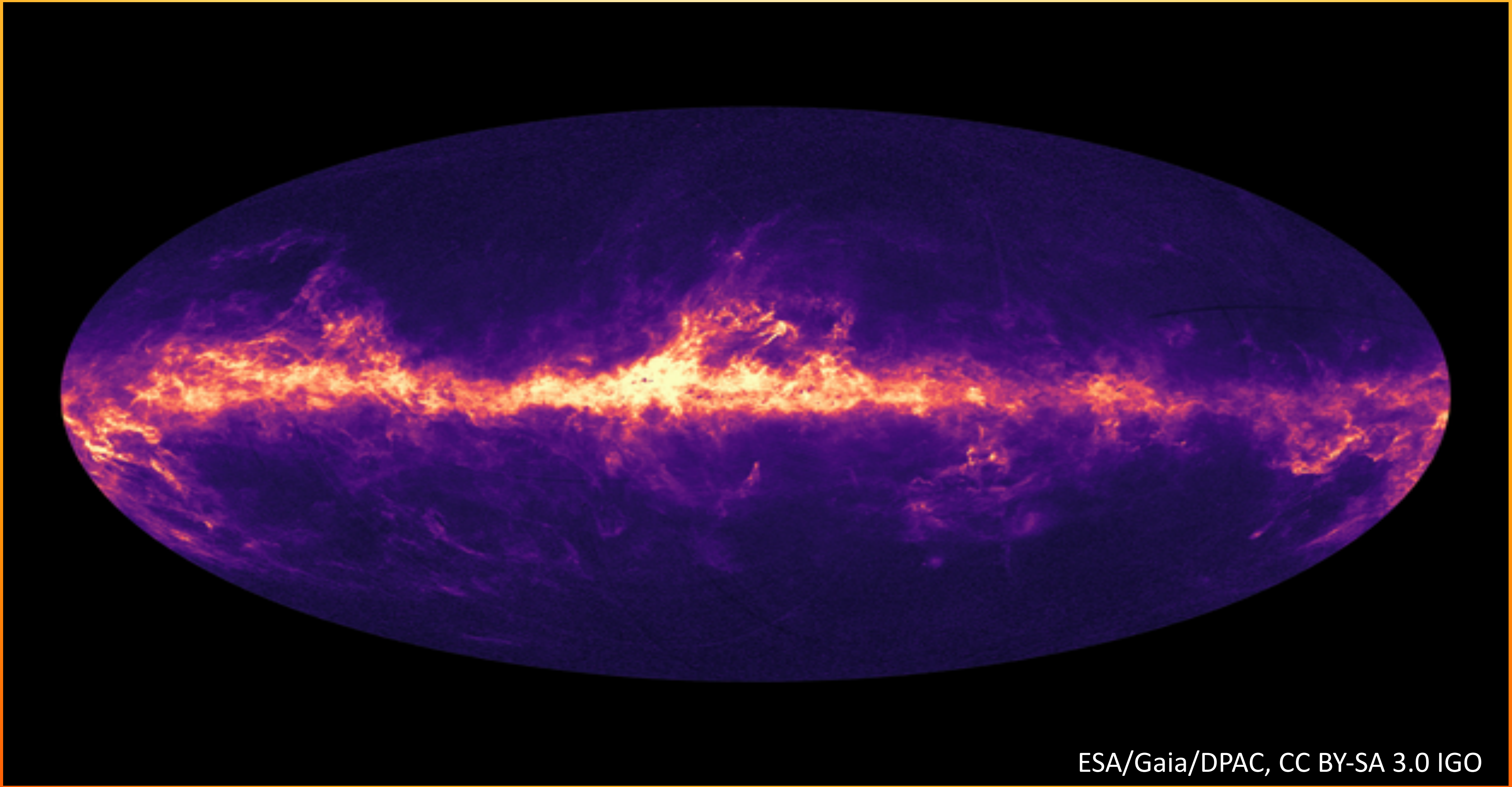

Dust Extinction and Dust Density Maps

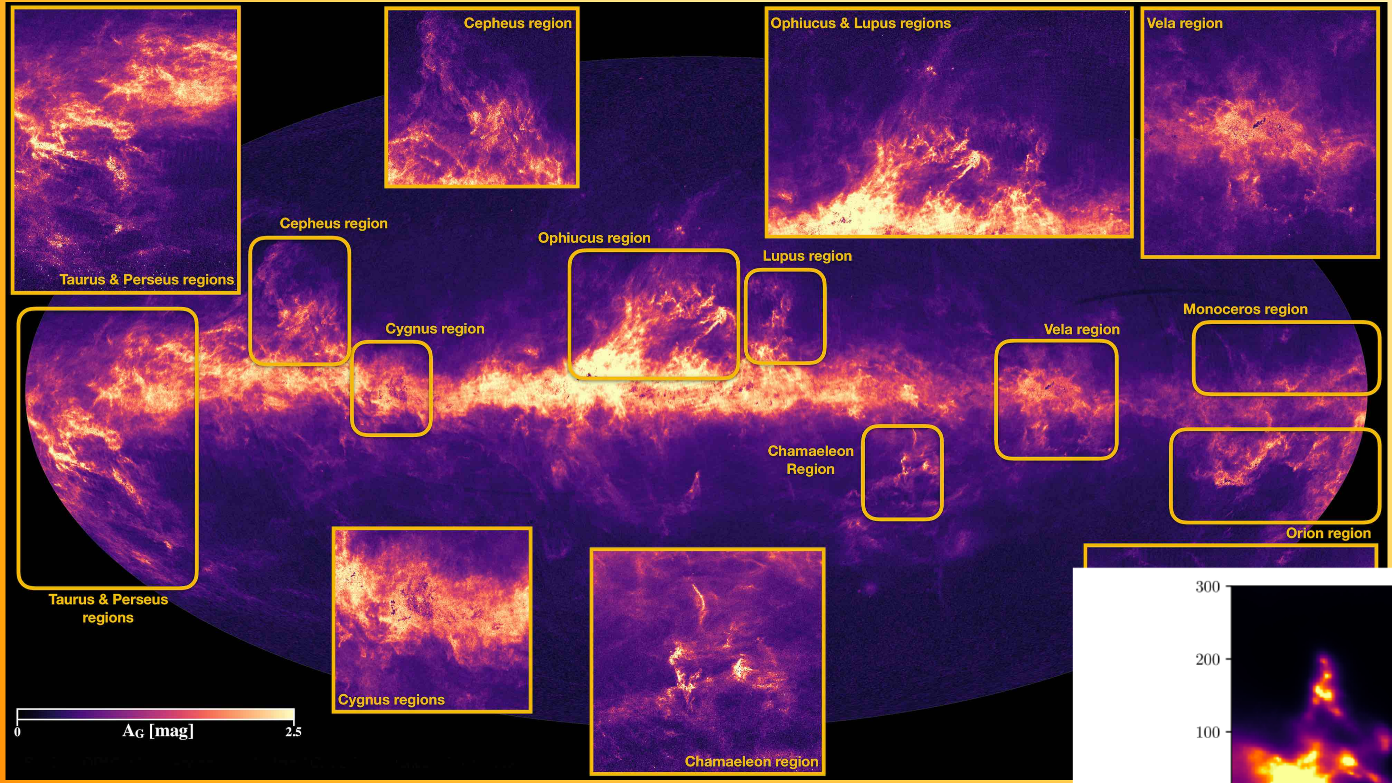

ESA/Gaia/DPAC, M. Fouesneau / R. Andrae / C.A.L Bailer-Jones of the Max Planck Institute for Astronomy (Heidelberg, Germany), O. Creevey of the Observatoire de la Côte d'Azur (Nice, France) and the entire CU8 team

Leike., et al., 2020

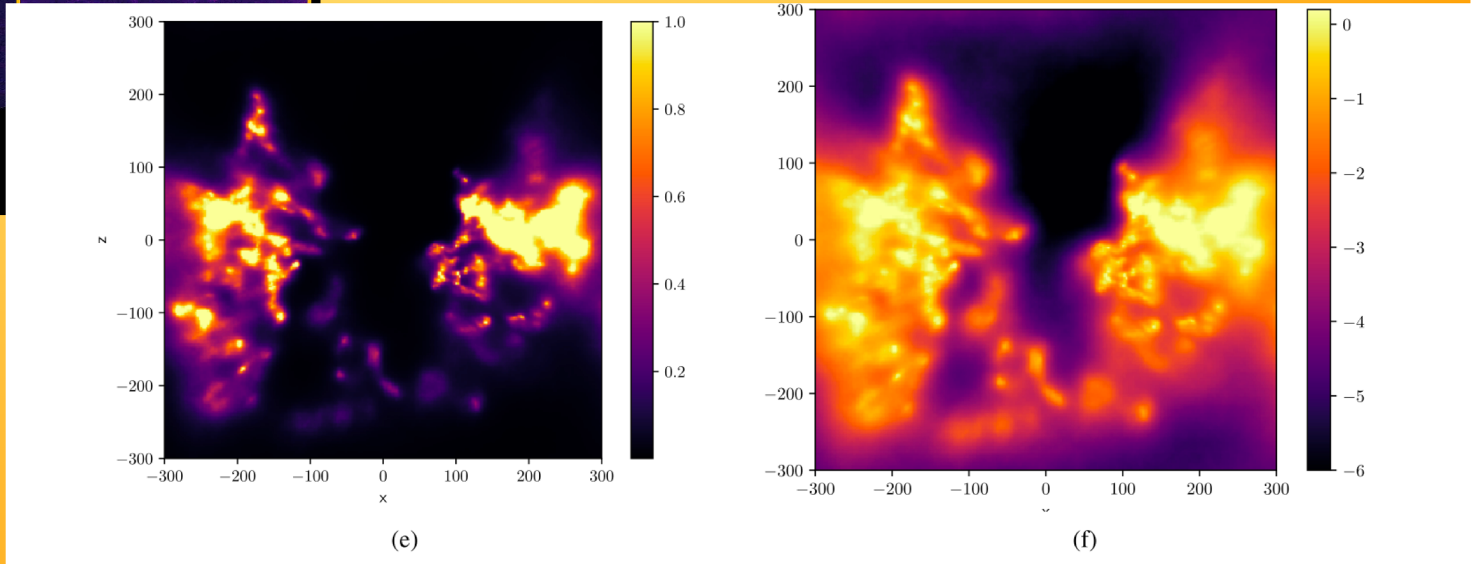

Fig. 13. Reconstructed dust density in different projections. The rows show integrated dust extinction for sightlines parallel to the z-, x-, and y-axis, respectively. In the first row, the Galactic center is located towards the left of the plot, in the other two rows the Galactic north is located towards the top of the plot. The cube is in Galactic coordinates, thus the x-axis is oriented towards the Galactic center and the z-axis is perpendicular to the Galactic plane. *First column*: integrated G-band extinction in e-folds of extinction, *second column*: logarithmic version of the first column.

Schlegel, Finkbeiner & Davis (1998)

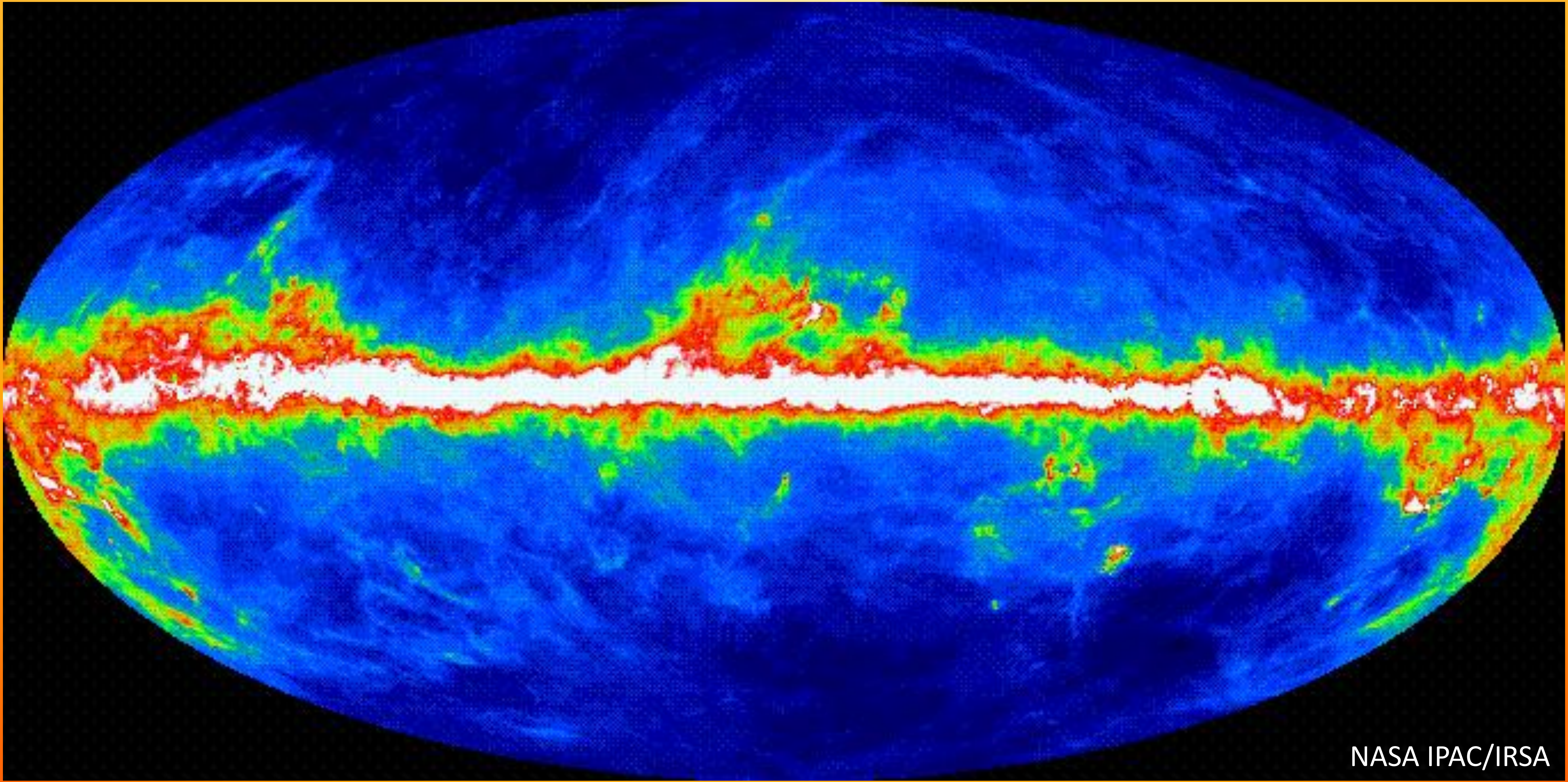

Many improvements in the last two decades using Gaussian processes and Bayesian inference

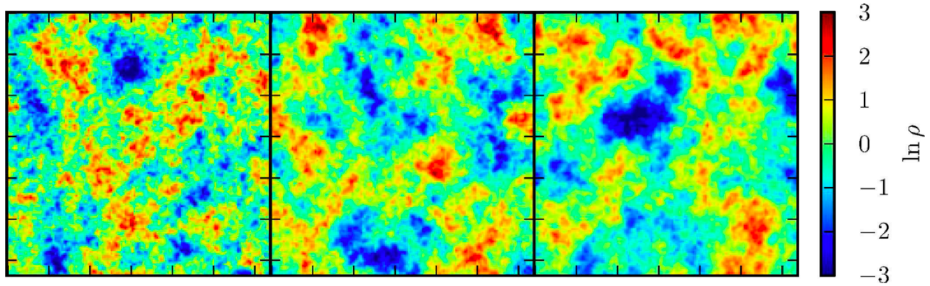

Figure B1. Slices through three lognormal random field cubes produced by exponentiating GRFs. On the left a field simulated assuming $\gamma = 3$, in the centre $\gamma = 3.5$ and on the right $\gamma = 4$.

Sale and Magorrian 2014

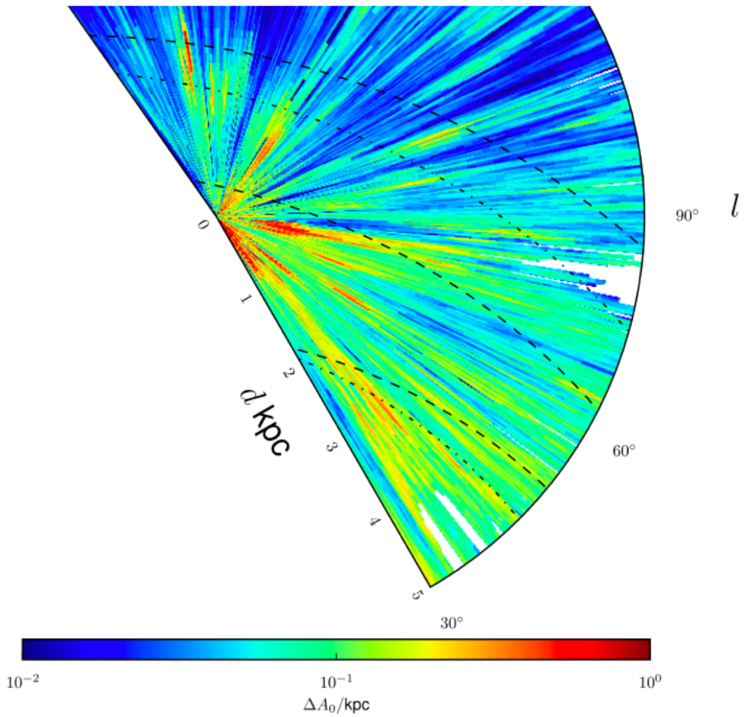

Figure 5. A map of extinction at $b = 0$, after convolution with a uniform kernel to reduce the resolution to 0.25° in l and 500 pc in distance, so as to roughly match the resolution of Figure 9 of Marshall et al. (2006). The sun lies at the plot's origin with the Galactic centre off the bottom of the plot. The dashed lines denote the position of the Sagittarius, local and Perseus spiral arms given by Reid et al. (2014), whilst the dot-dashed lines correspond to the Sagittarius and Perseus arms of Vallée (2013). Note the nonphysical 'fingers of God' – discontinuities in the azimuthal direction.

Sale et al., 2014

Green et al., 2015

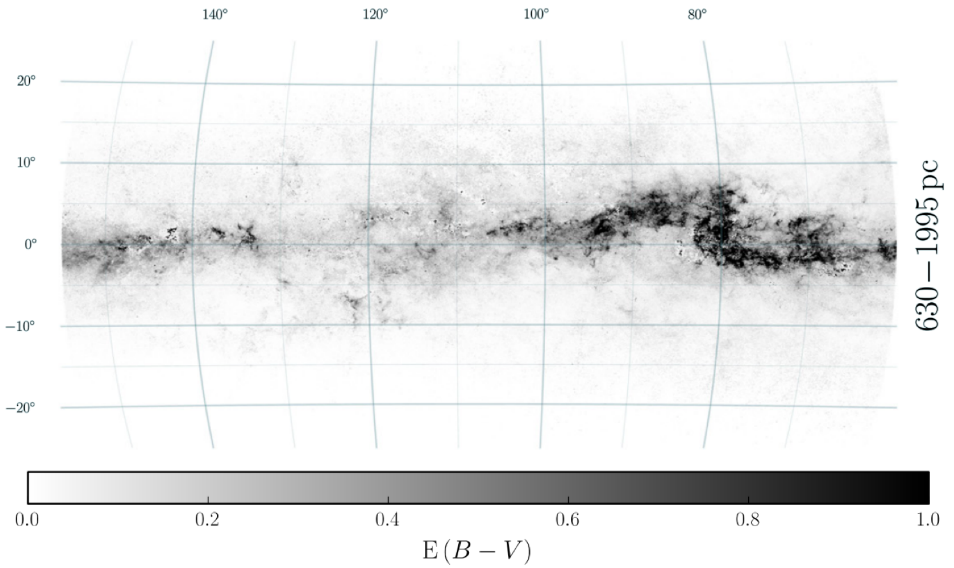

Figure 7. Closer view of the dust in the direction of Cepheus and Polaris flares and the eastern portion of the Great Rift, including Cygnus X. The Cepheus flare ($95° \lesssim \ell \lesssim 110°$, $b \approx 15°$) separates into two components in distance, visible in the first and third panels. The dust associated with the Cygnus X region ($\ell \approx 80°$, $b \approx 0°$) appears in the third panel.

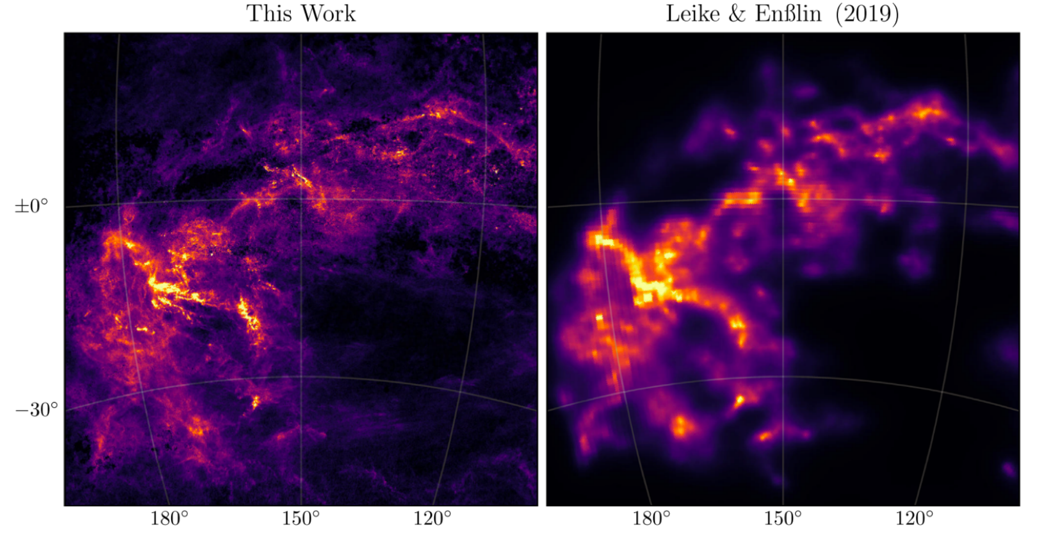

Figure 13. Comparison with Leike & Enßlin (2019) in the Galactic anticenter. Reddening density is integrated out to a distance of 300 pc, and displayed in arbitrary units.

Green et al., 2019

Many improvements in the last two decades using Gaussian processes and Bayesian inference

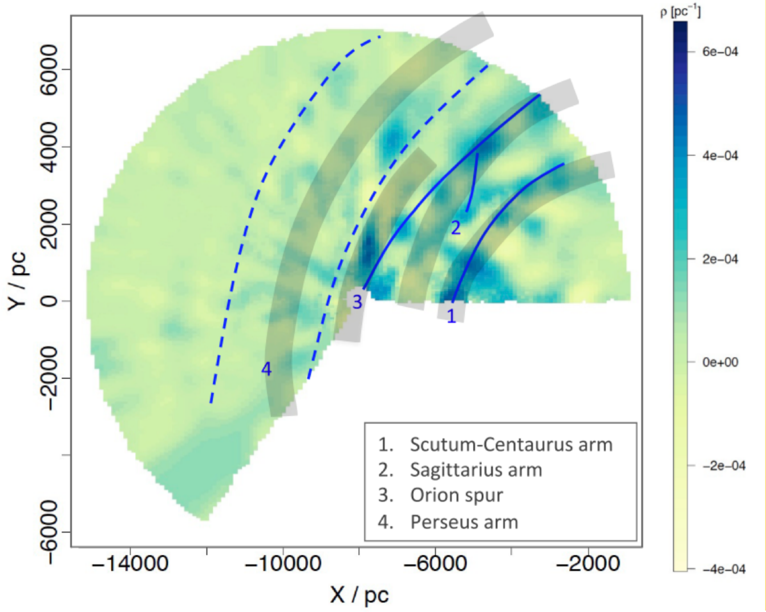

Fig. 7. As Fig. 4 left, but overplotting spiral arms model from Reid et al. (2014) as grey shaded curves. The width of the shaded curves is equal to 2σ uncertainty in the arm fitting (1σ on each side of the central curve, Reid et al. 2014).

Rezaei Kh., et al., 2019

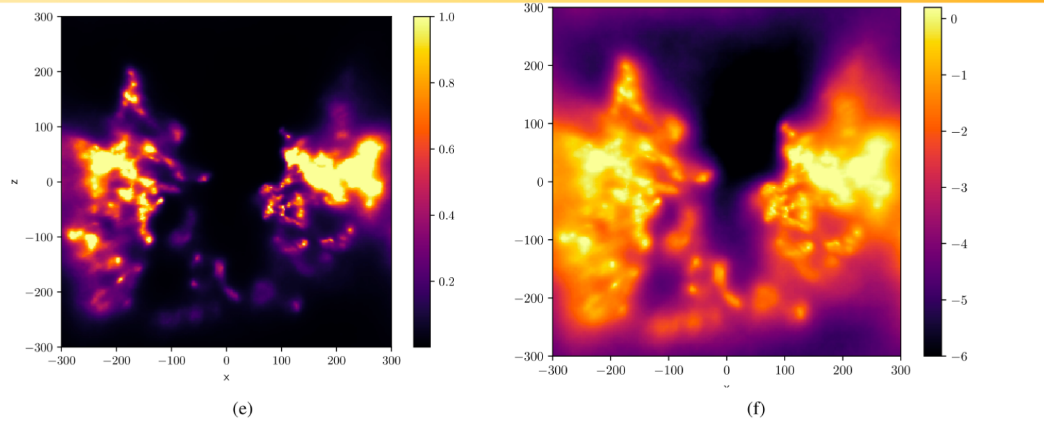

Fig. 13. Reconstructed dust density in different projections. The rows show integrated dust extinction for sightlines parallel to the z-, x-, and y-axis, respectively. In the first row, the Galactic center is located towards the left of the plot, in the other two rows the Galactic north is located towards the top of the plot. The cube is in Galactic coordinates, thus the x-axis is oriented towards the Galactic center and the z-axis is perpendicular to the Galactic plane. *First column*: integrated G-band extinction in e-folds of extinction, *second column*: logarithmic version of the first column.

Leike., et al., 2020

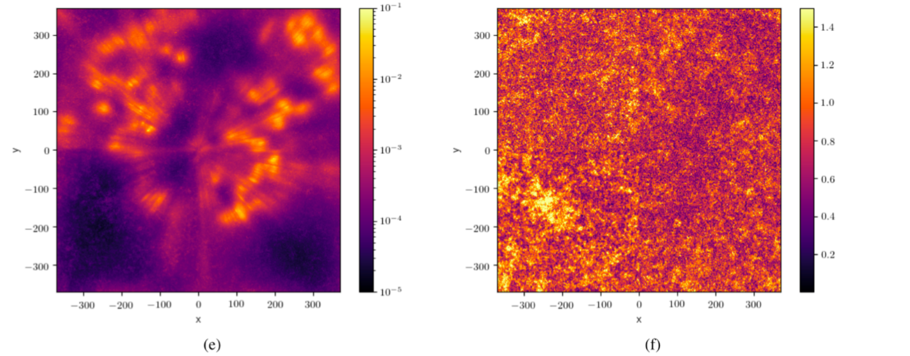

Fig. 2: Result of our 3D dust reconstruction. The first column shows dust extinction, the second shows the relative error. The first row shows the integrated extinction in e-folds in a Mollweide projection of the whole reconstructed box of 740 pc × 740 pc × 540 pc. The second row also shows integrated extinction in e-folds in the same box, but integrated normal to the Galactic plane instead of radially. The third row shows differential extinction in e-folds per parsec in a slice along the Galactic plane.

Leike., et al., 2019

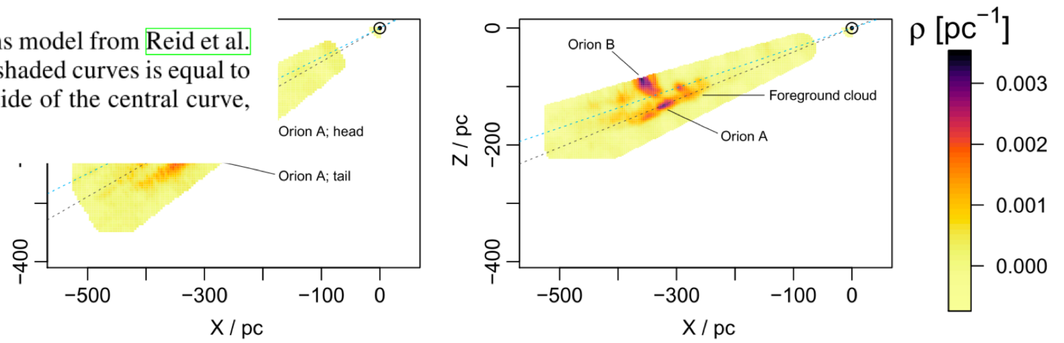

Fig. 1. Two Cartesian projections of the 3D dust distributions in Orion. The Sun is at (X, Y, Z) = (0 , 0, 0), with X increasing towards the Galactic centre and Z points to the North Galactic pole, perpendicular to the Galactic disk. The left panel looks through the Galactic plane from north to south and the right panel is perpendicular to that of the left, having the Galactic height as the vertical axis. The presence of the foreground bubble structure is evident in both projections. Also the extent of the tail of Orion A to large distances is clearly seen from the left panel. The dashed lines are two l.o.s passing through different parts of the foreground cloud analysed further in Fig 3. The predictions are made on regular grids for every 0.5 degrees in the Galactic l and b, and every 10 pc in distance. The 2D image is then produced by applying a smoothing kernel (with 4-pc scale length) to handle the missing pixels. In order to not produce extra smoothing than that of the method, the length scale of the kernel is chosen to be relatively small; hence, the distance gridding is still apparent in the left panel.

Rezaei Kh., et al., 2018

Challenges and Issues mapping the 3D dust density

- Fingers-of-god effects: dust distribution is elongated along the lines-of-sight due to higher tangential than radial accuracy.
- Maintaining the physical requirement that densities be positive and hence extinction must be monotonically increasing along any line-of-sight.
- Computationally intensive, especially GP methods

- High accuracy distances are available and/or if correlations between points in 3D space are incorporated explicitly rather than as individual lines-of-sight coupled together in the plane of the sky.
- Model the logarithm of the density instead of density or extinction itself
- Methods with improved scaling are therefore important to ensure that a wide range of problems are feasible with minimal trade-offs between, for example, resolution, map size, and number of sources

Our solution - novel method!

- A combination of latent variable GPs combined with variational inference – Flexible and Non parametric

Latent variable GPs

- Latent variable GPs – A layered GP where we fit model predicted extinction to observed extinction at the top level while inferring the 3D density directly in the bottom layer

- We predict a full density map with each iteration - Correlations between points in 3D space are incorporated explicitly rather than as individual lines-of-sight coupled together in the plane of the sky

- Maps $\log_{10}(\boldsymbol{\rho})$ instead of $\boldsymbol{\rho}$
Maintains the physical requirement that densities be positive and hence extinction must be monotonically increasing along any line-of-sight.

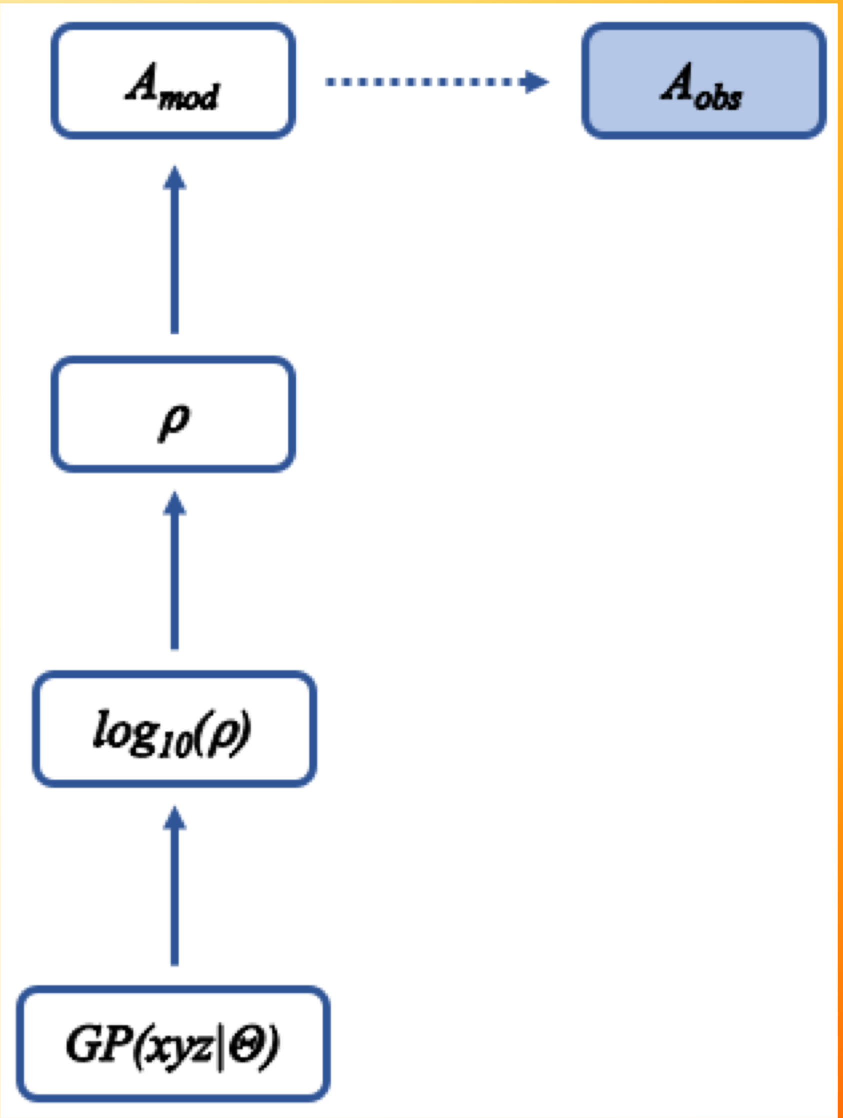

Variational inference

- Replaces the target posterior of the GP with an approximate posterior that is easier to work with, and finds the parameters for this approximation that best reproduce the true posterior

- Reduce the dimensionality of the problem by conditioning the GP only on a subset of points, known as the inducing points

- Improved scaling with minimal trade-offs between, resolution, map size, and number of sources.

Implementation

- Train and predict on separate grids
- GP optimised using ELBO via ADAMW algorithm

Built entirely on publicly available python packages

- Gpytorch (Gardner et al. 2018), Pyro (Bingham et al. 2018; Phan et al. 2019)
- Reproducible and open source

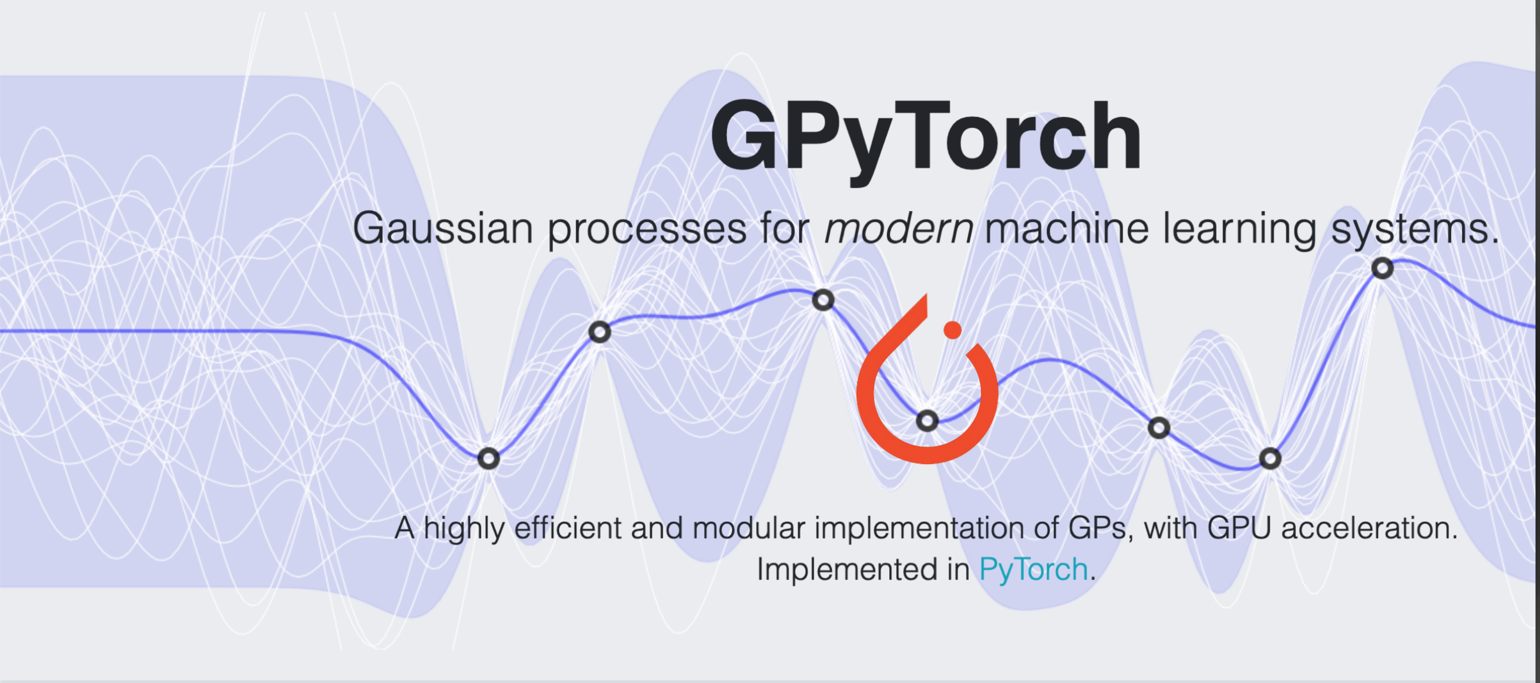

Input data – Catalogue of APs by Fouesneau et al., in prep.

- Uses Gaia, 2MASS, WISE photometry to predict APs
- Our input parameters: Extinction A_0 and uncertainties, Distance and uncertainties, l and b coordinates
- Jointly estimates distance with the extinction. Do not rely on the inverse parallax as distance measurements. Obtain a coherent set of input data

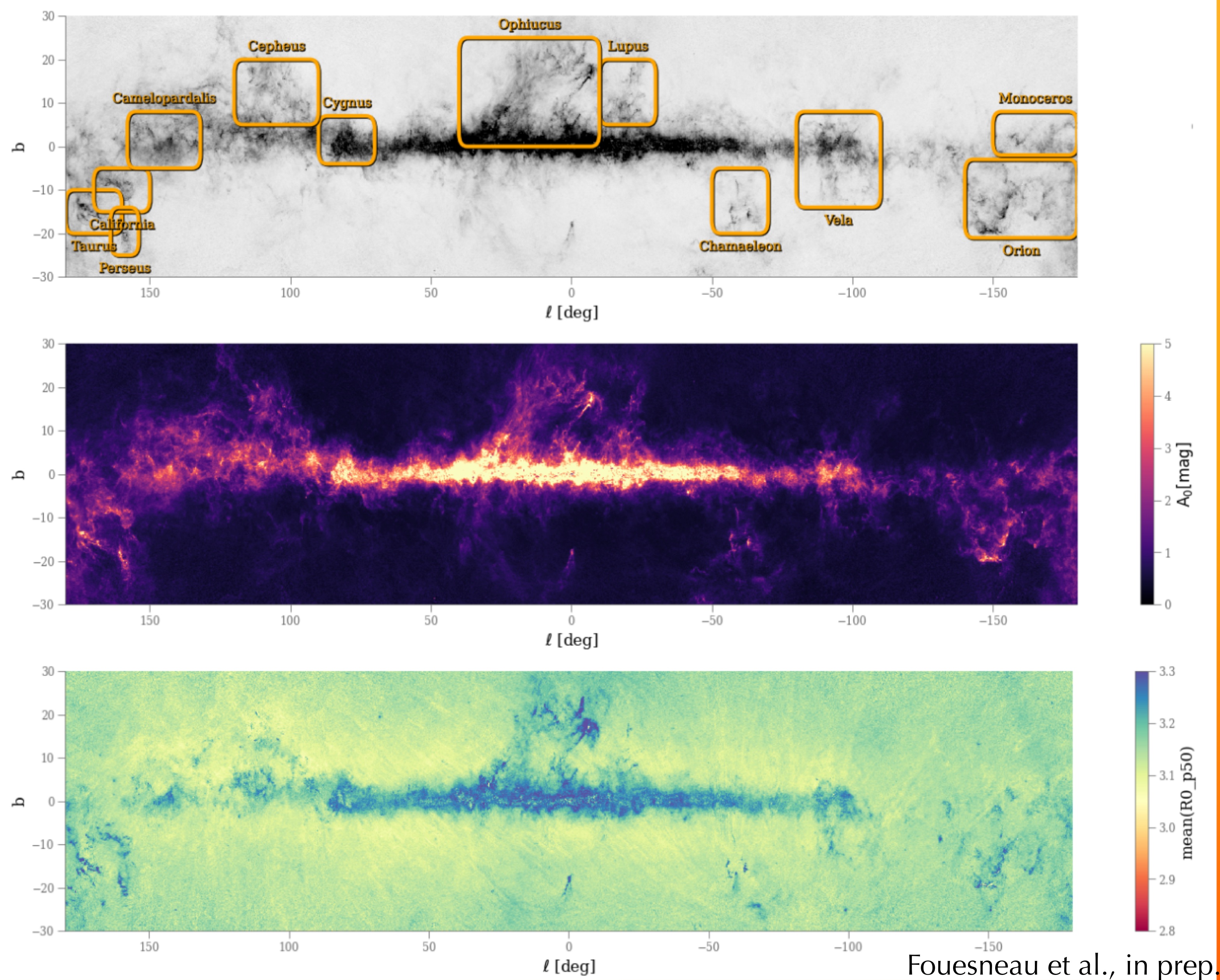

Fouesneau et al., in prep.

Input data – Catalogue of APs by Fouesneau et al., in prep.

- Achieve more reliable estimates of stellar parameters by combining multiple spectroscopic and photometric surveys

- IR indicators such as RJCE (Majewski et al. 2011) optimized for particular applications, are less sensitive to column density than optical bands. Not recommended for use on non-giant stars

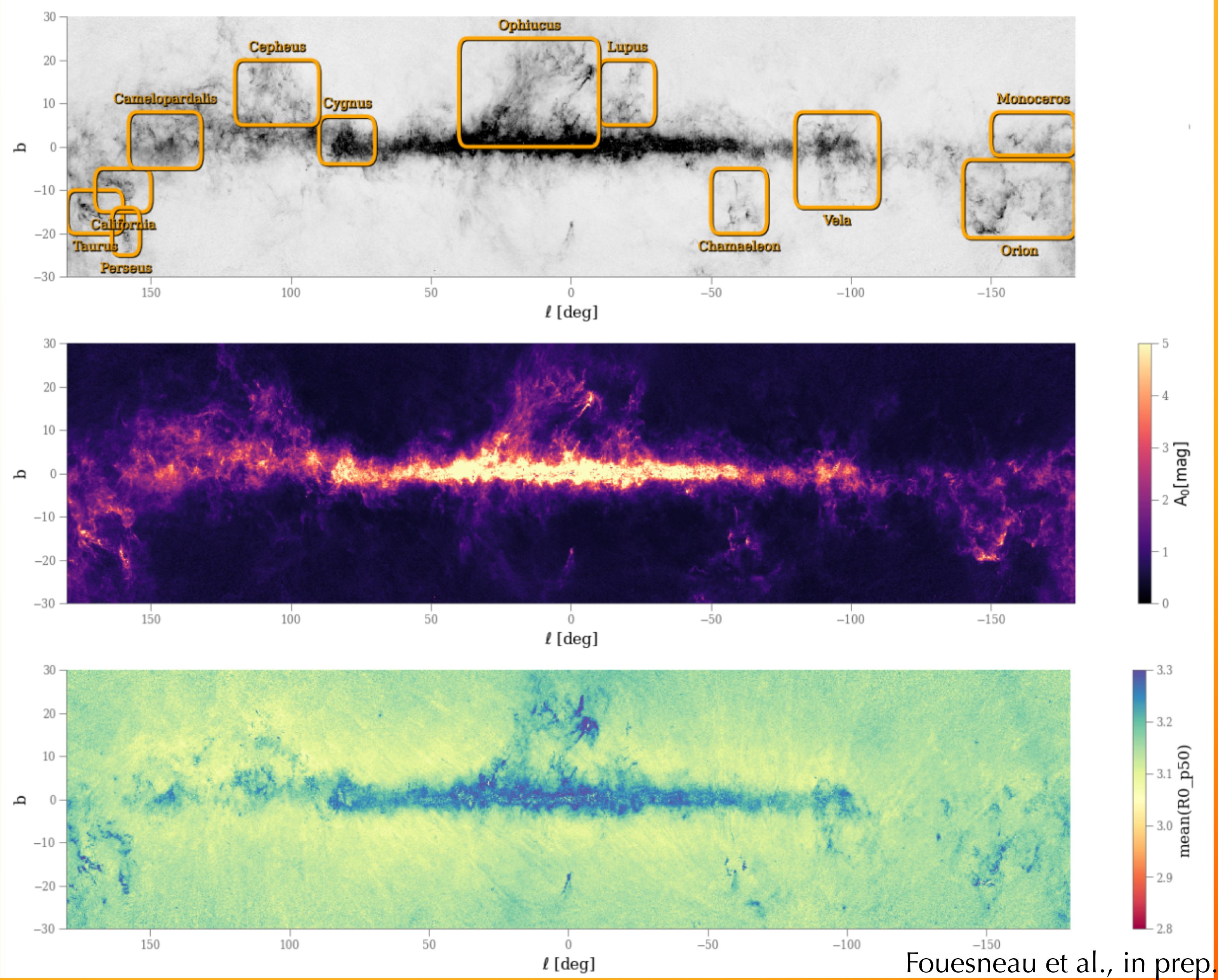

Fouesneau et al., in prep.

Applying our method to SFRs Orion, Cygnus X, Perseus and Taurus

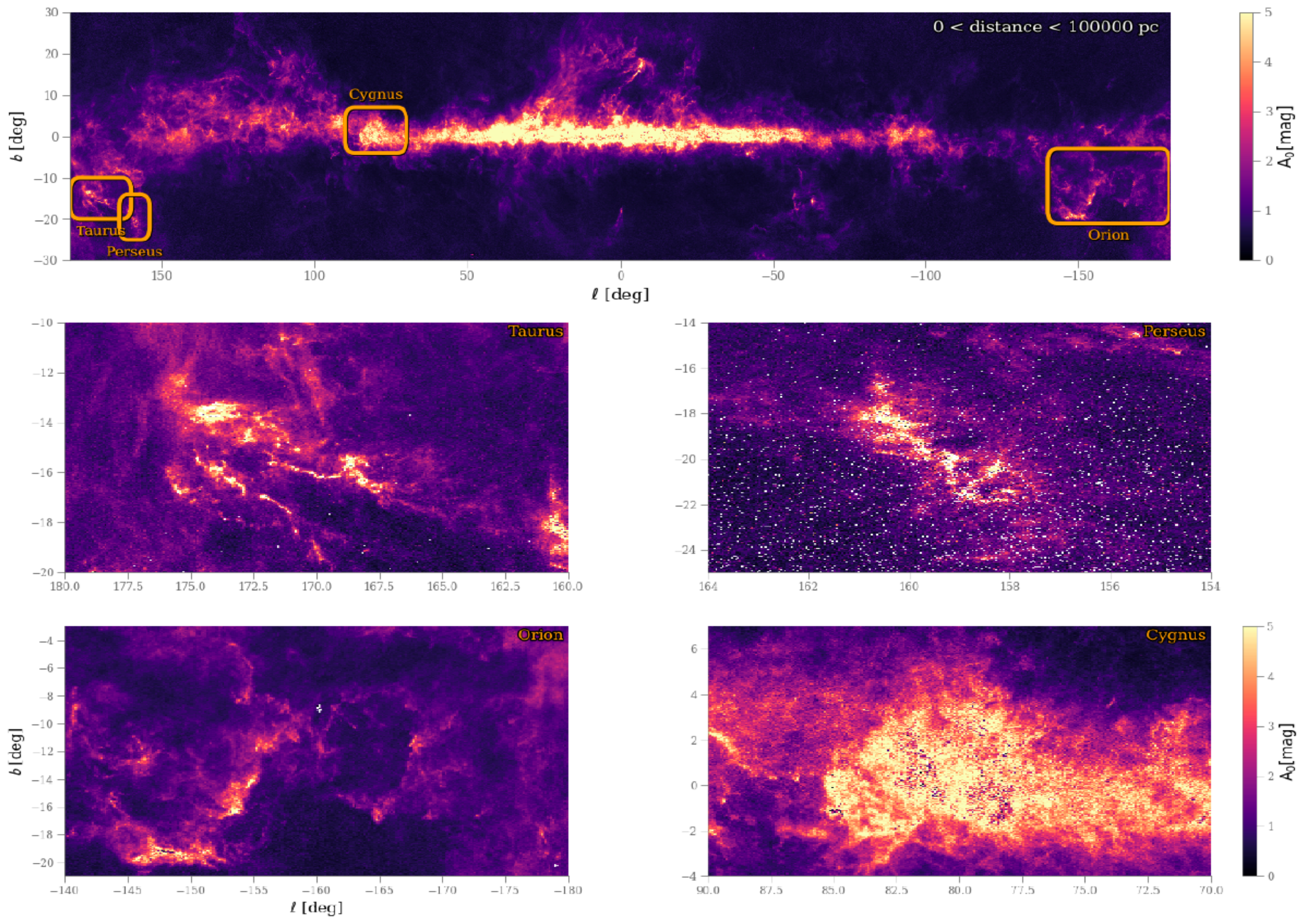

Fig. 6: Extinctions as a function of Galactic coordinates from the catalogue of Fouesneau et al. (in prep) with the star formation regions analysed in this paper highlighted. *Top*: Full Galactic extinction map; *Middle left*: Taurus; *Middle right*: Perseus; *Bottom left*: Orion; *Bottom right*: Cygnus X

Dharmawardena et al., subm. A&A

Orion

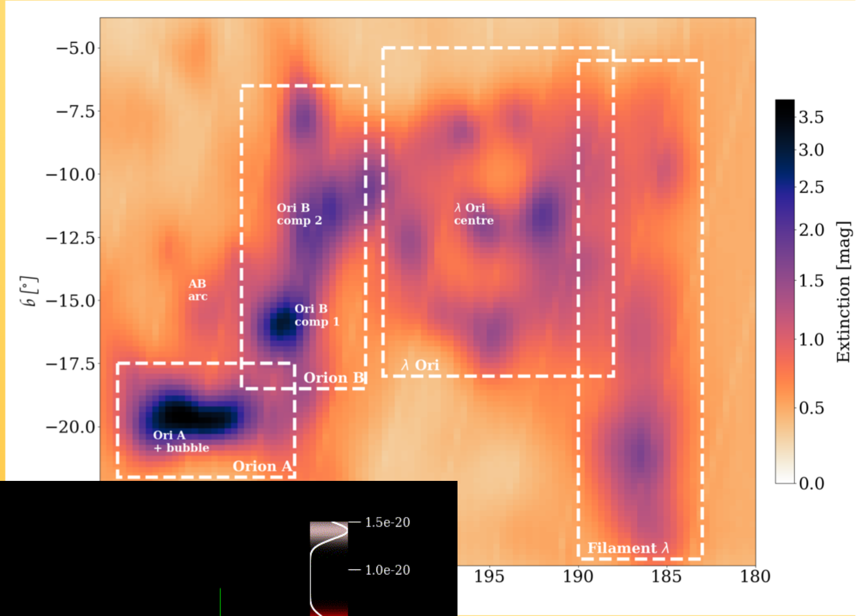

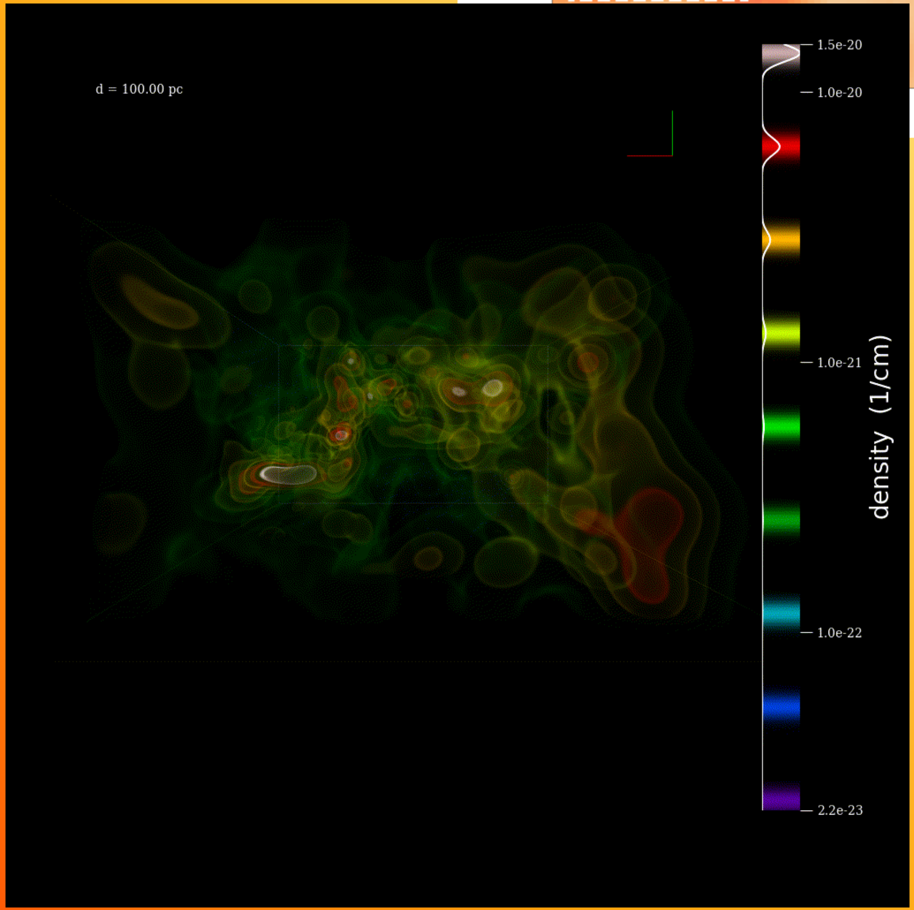

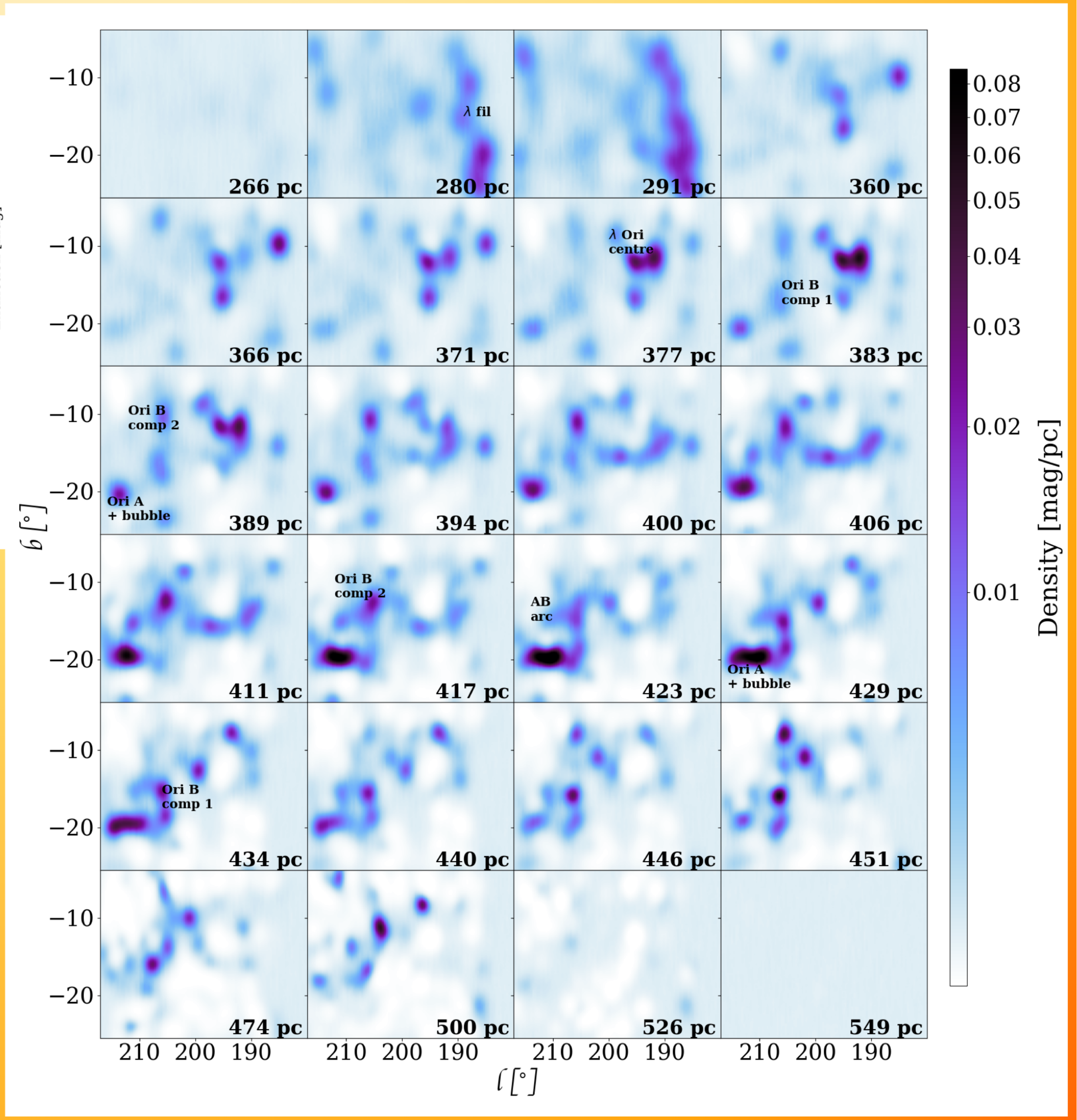

Dharmawardena et al., subm. A&A

Cygnus X

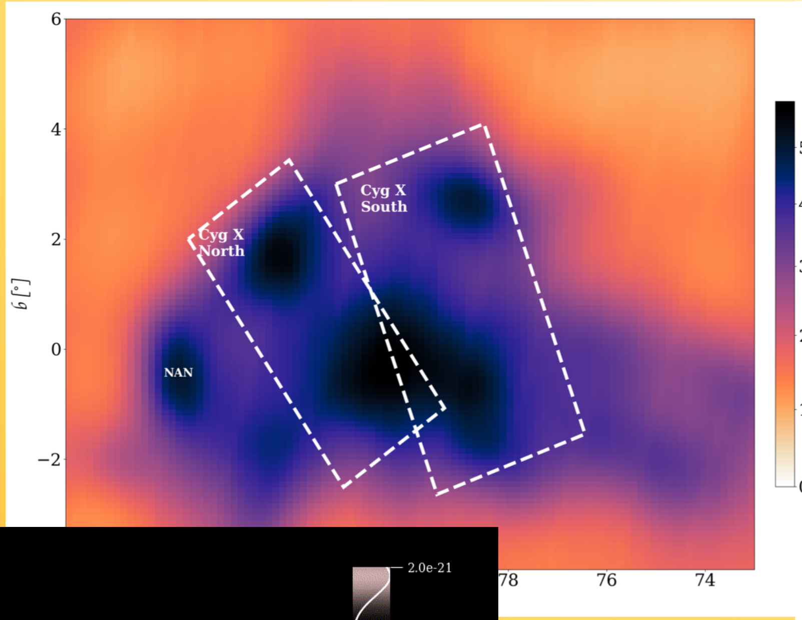

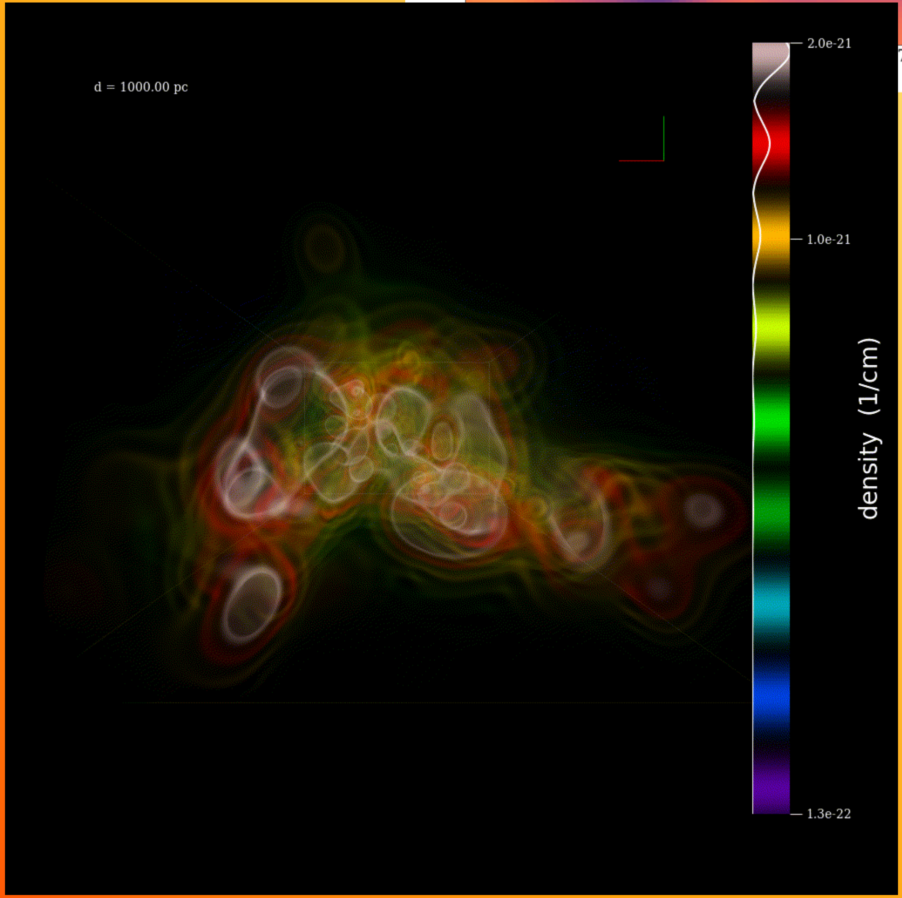

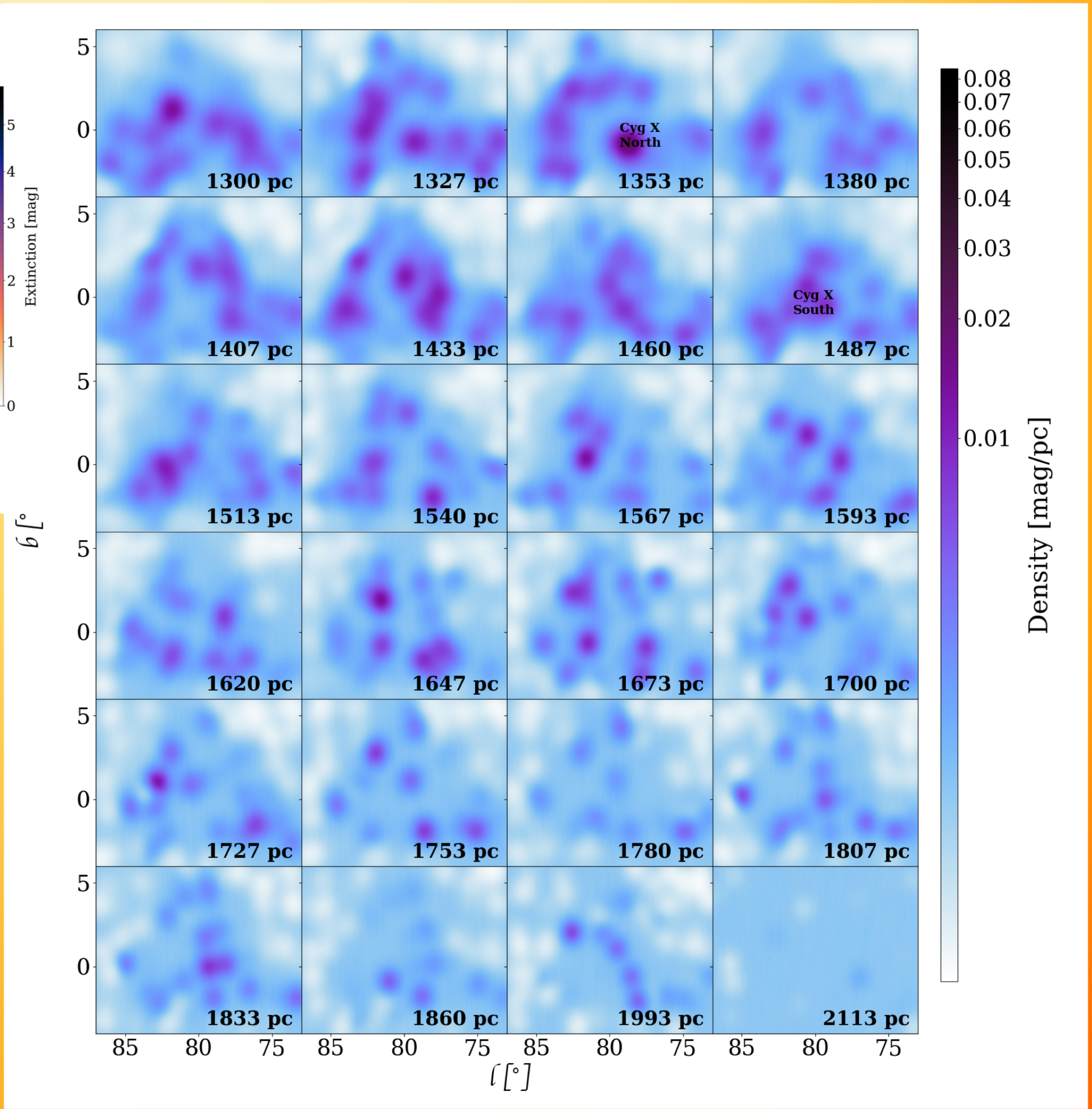

Dharmawardena et al., subm. A&A

Perseus

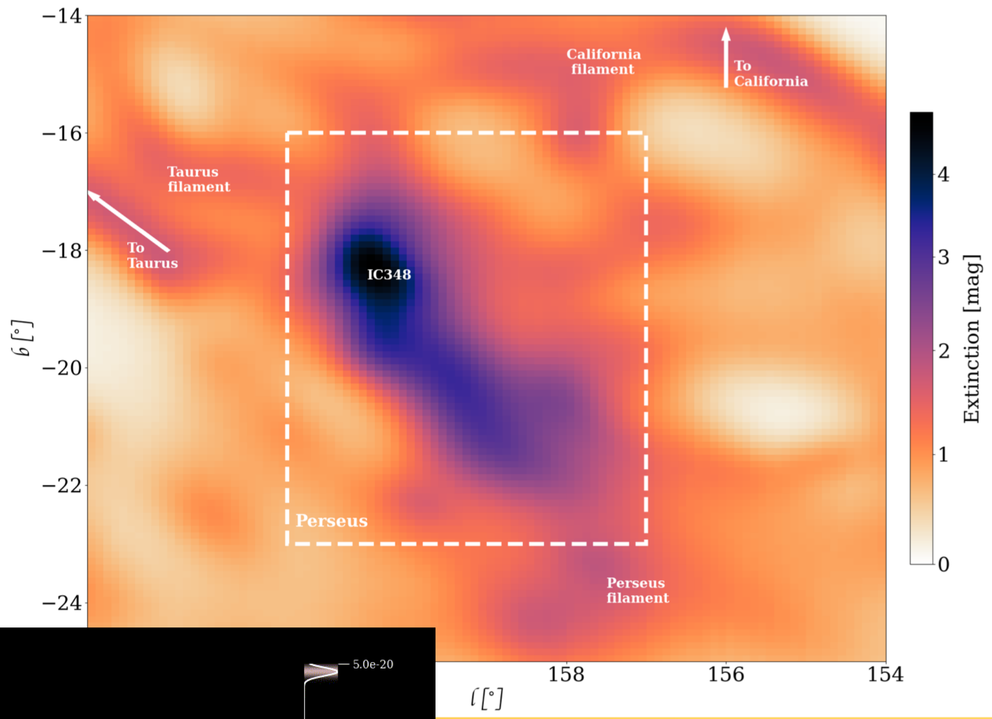

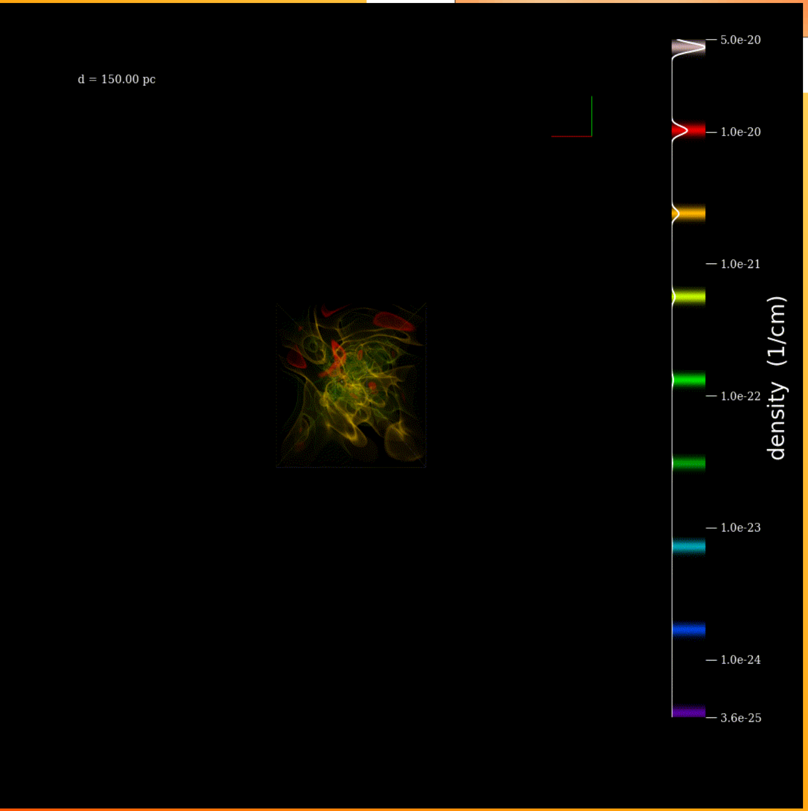

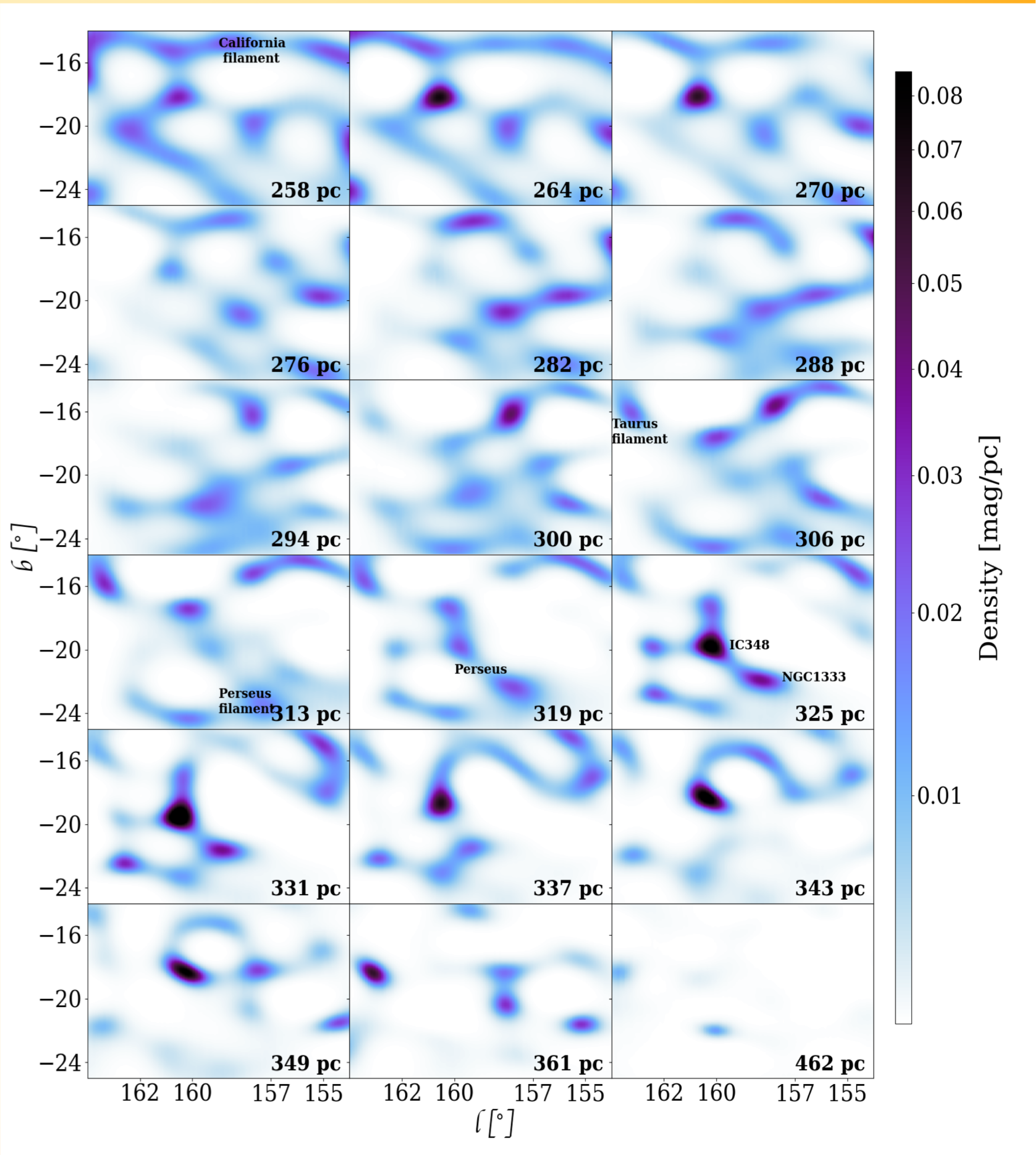

Dharmawardena et al., subm. A&A

Taurus

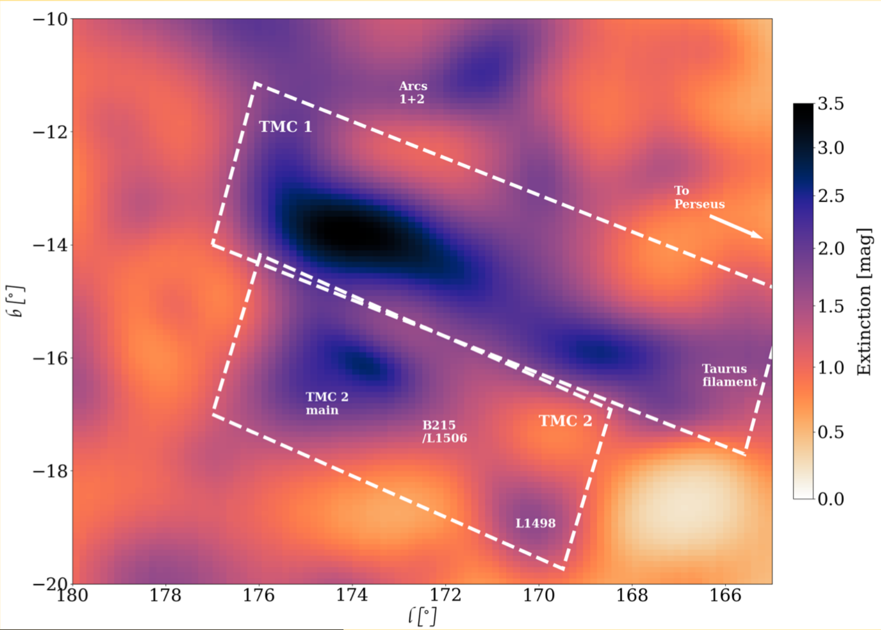

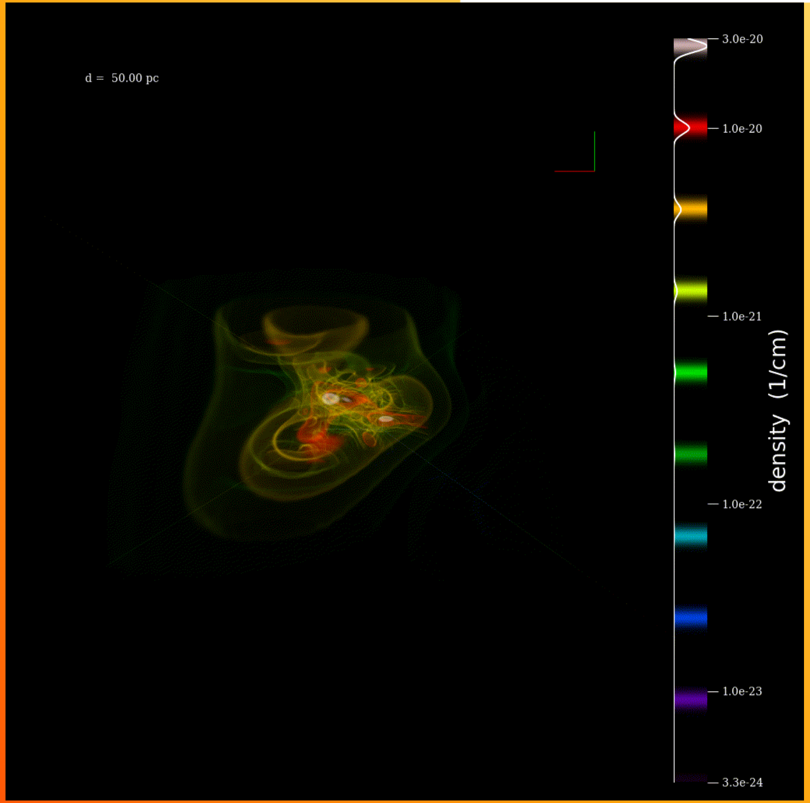

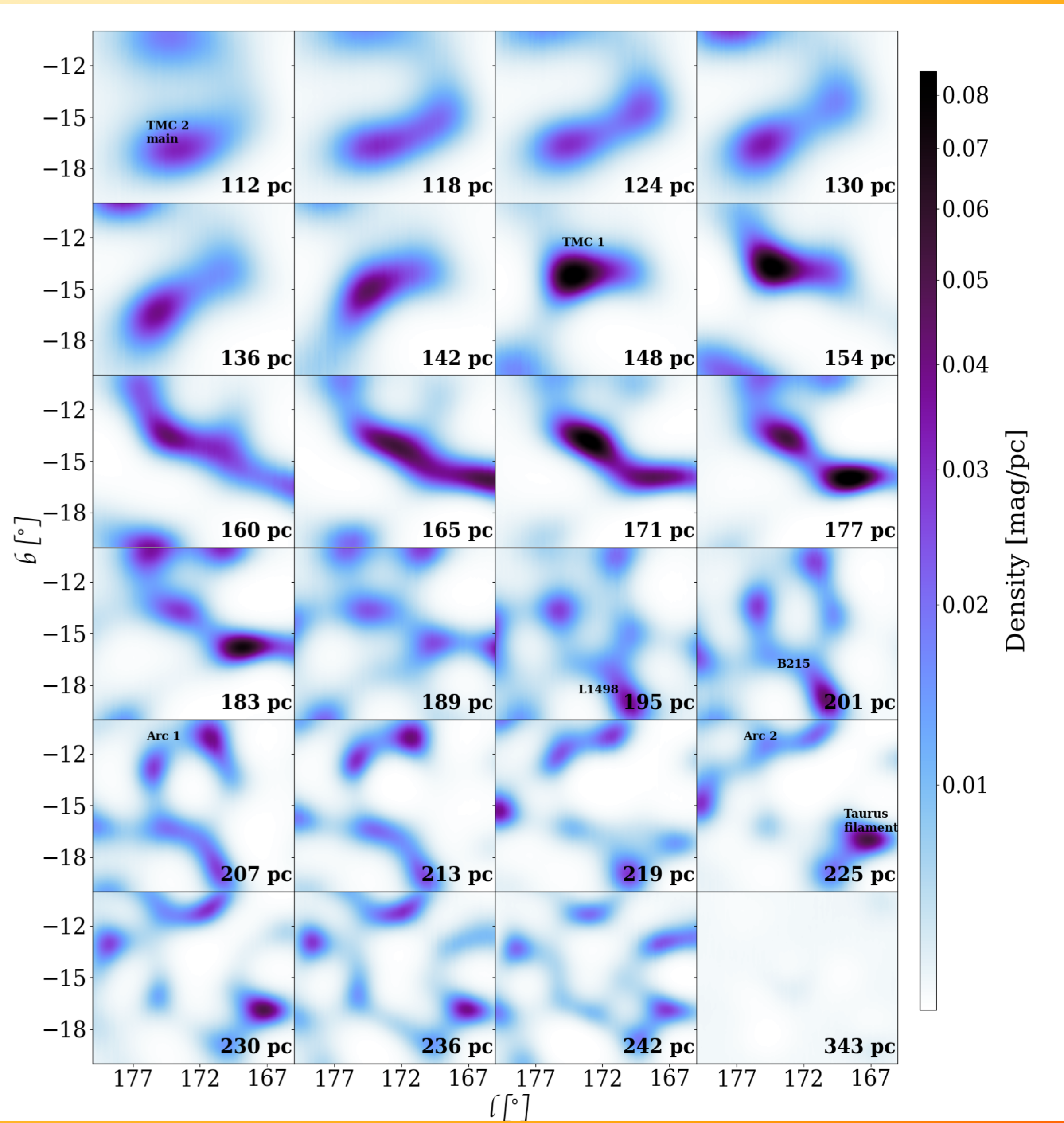

Dharmawardena et al., subm. A&A

Dust Mass

$$M_d = d_{max}^2 \int_{b_{min}}^{b_{max}} \cos b \, db \int_{l_{min}}^{l_{max}} dl \, \frac{A_{\mathrm{mod,d_{max}}}(l,b)}{1.086\kappa_0}$$

- Dust opacity κ_0 and dust:gas ratio derived from Draine et al., 2003 A and B

Region	Dust Mass ($10^3 M_\odot$)	Total Mass ($10^3 M_\odot$)
Orion	$9.1^{+3.2}_{-2.2}$	1130^{+400}_{-270}
Cygnus	$88.2^{+7.0}_{-6.2}$	10900^{+900}_{-800}
Perseus	$1.5^{+0.1}_{-0.1}$	187^{+17}_{-14}
Taurus	$1.2^{+0.1}_{-0.1}$	149^{+17}_{-14}

Dharmawardena et al., subm. A&A

Comparison to Planck

Dharmawardena et al., subm. A&A

- Compare Planck sub-mm optical depth of dust at 353 GHz (τ_{353}) to our cumulative extinctions

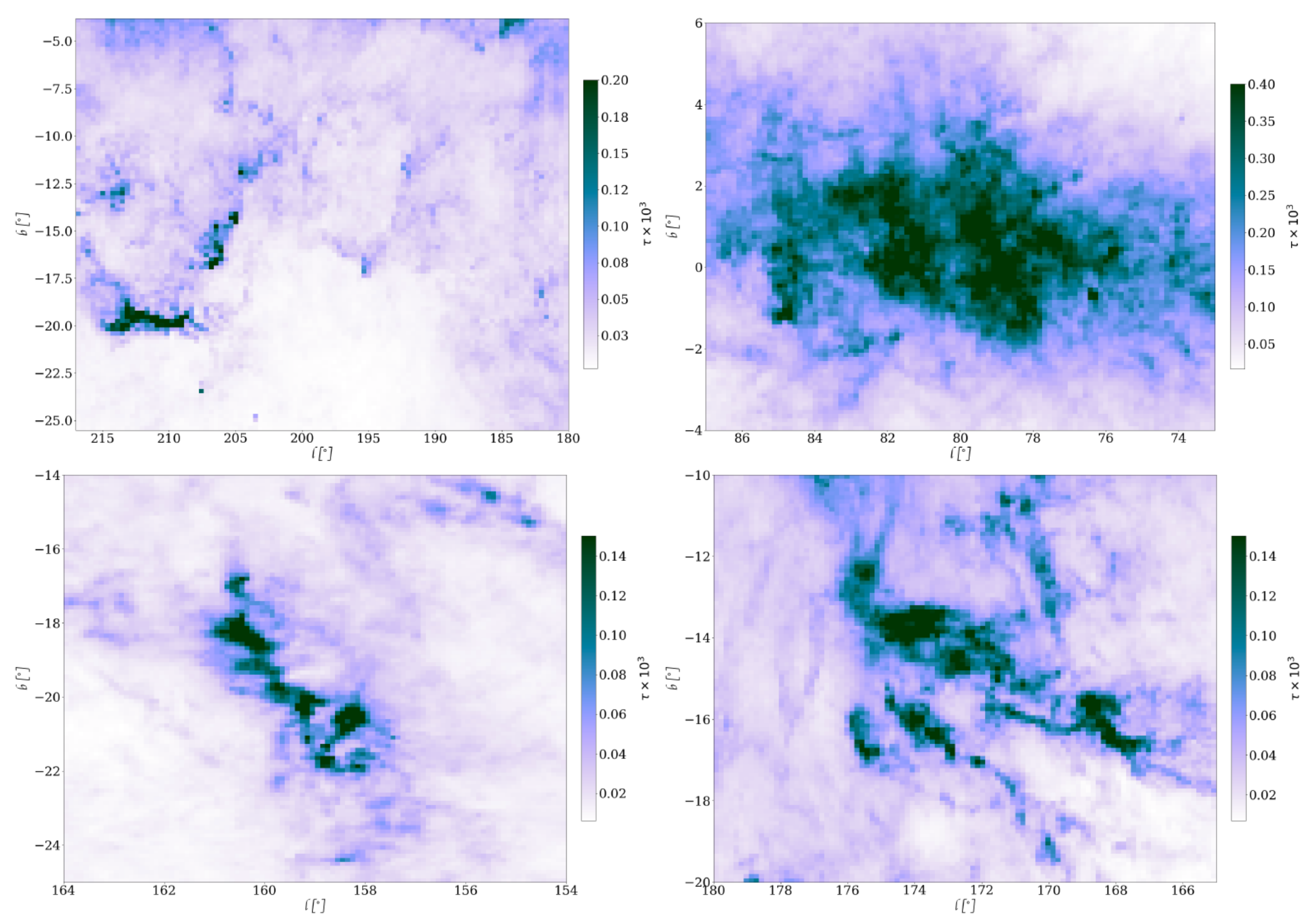

Comparison to Planck

Dharmawardena et al., subm. A&A

- Ratio of Planck τ_{353} compared to our cumulative extinctions – normalised by median of ratio

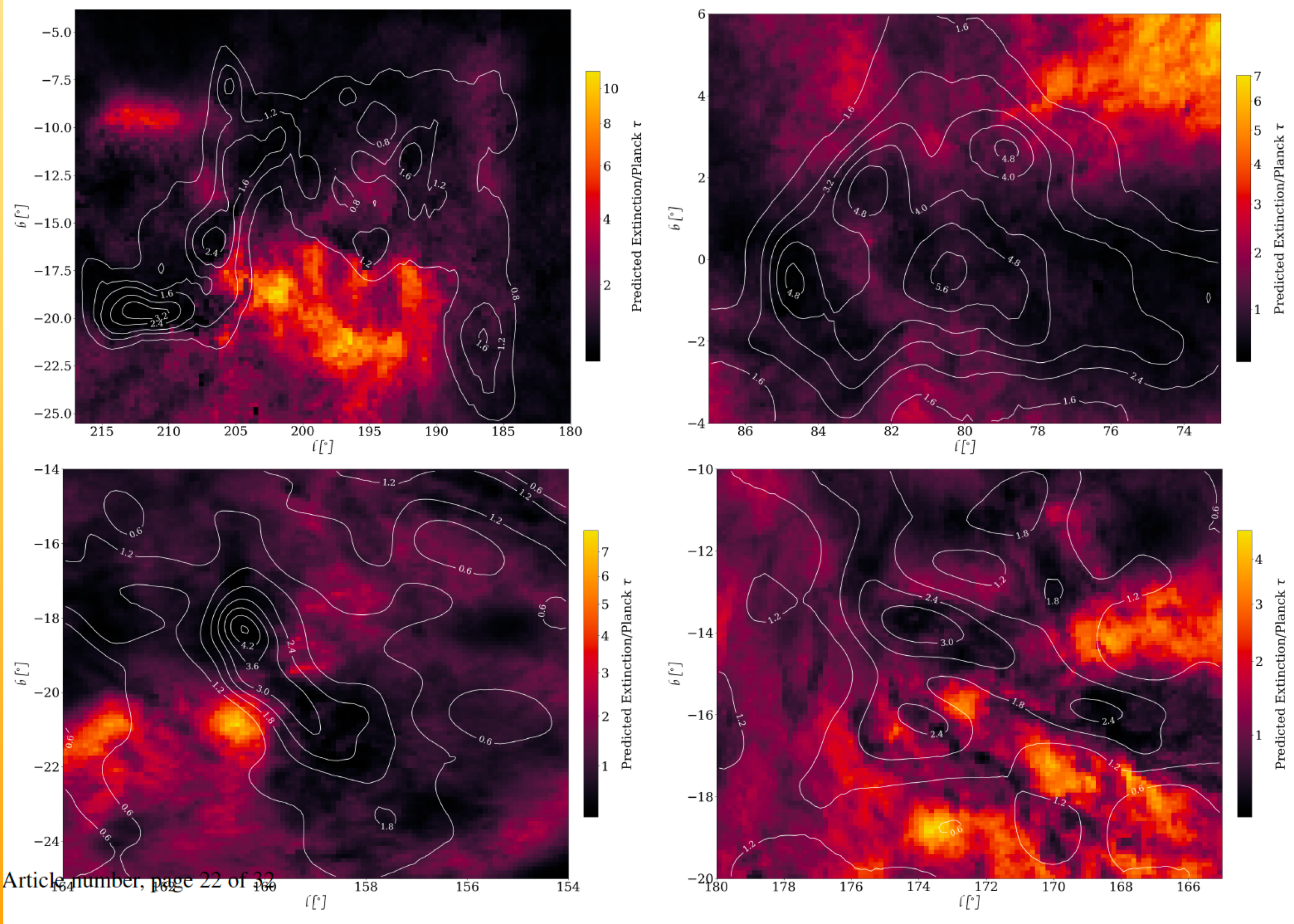

Applications for our maps

- Extend to the full MW

- Compare stellar densities to dust densities on clump scales – what will it tell us about star-formation rates, etc or on a wider MW scale

- Compare with gas observations to measure regional dust:gas ratios

- Only a few examples.. so much more! Please contact us if you'd like to use our maps.